Supporting Information

A series of terpyridine-based zinc(II) complexes assembling for third-order nonlinear optical response in the near-infrared region and recognizing lipid membranes

Yiwen Tang,[a] Ming Kong,[a] Xiaohe Tian, [b] Dandan Li,[a] Hui Liu,[a] Jinghang Wang,[c] Qiong Zhang*[a], Hongping Zhou,[a] Jieying Wu[a] and Yupeng Tian[a, d]

[a]Department of Chemistry, Key Laboratory of Functional Inorganic Material Chemistry of Anhui Province, Anhui University, Hefei 230039, P. R. China

[b]School of Life Science, Anhui University, Hefei 230039, P. R. China.

[c]School of Chemistry and Chemical Engeering, Huangshan University, Huangshan, P. R. China

[d]State Key Laboratory of Coordination Chemistry, Nanjing University, Nanjing 210093, P. R. China

*Corresponding author: zhangqiong.314@163.com; jywu1957@163.com; yptian@edu.ahu.cn

Content

Experimental Section

2.2.5 Crystallography

The single crystal X-ray diffraction measurements were performed on Bruker Smart 1000 CCD area detector diffractometer. The determination of unit cell parameters and data collections were performed with Mo-Kα (λ=0.71073 Å). And all structures were solved by direct methods and difference Fourier syntheses. The non-hydrogen atoms were refined anisotropically and hydrogen atoms were introduced geometrically. The final refinement was performed with SHELXTL-97 program package. To deeply understand the relationship between molecule geometry and optical property, we tried to obtain as many as single-crystal structures of our compounds. The crystal data collection and refinement parameters are given in **Table S1**.

2.2.6 Computational details

Optimizations were performed on B3LYP [LANL2DZ] without any symmetry restraints, and the TD-DFT {B3LYP[LANL2DZ]} calculations were carried out with the crystal structure or the optimized structure. All calculations, including optimizations and TD-DFT, were performed using the G03 software. Geometry optimization of singlet-singlet excitation energies were carried out with a basis set composed of 6-31G(d) for C, N, O, Cl, Br, I and H atoms and the LANL2DZ basis set for Zn atoms. The basis set was downloaded from the EMSL basis set library. The lowest 25 spin-allowed singlet-singlet transitions were taken into account in the calculation of the absorption spectra (Frisch et al., 2004).

2.2.7 Third-order NLO properties

To study the third-order NLO properties of **Z1**-**Z4**, their nonlinear absorption coefficient (β) and 2PA cross section (δ) were obtained by an open-aperture Z-scan technique using a femtosecond laser pulse (680-1080 nm, 80 MHz). The pulse length was 140 fs, the thermal heating of the sample with high repetition rate laser pulse was removed by the use of a mechanical chopper running at 10 Hz, and the average laser power was 36 mW. The sample in DMSO (its thickness is 1 mm) was put in the light path, and all measurements were carried out at room temperature (Zhang et al., 2014). The filled squares represent the experimental data, and the solid line is the theoretical curve modified from the following equations (Zhang et al., 2014; Xiao et al., 2015):

$$T(z, s = 1) = \sum_{m=0}^{\infty} \frac{[-q_0(z)^m}{(m+1)^{3/2}};\ q_0(z) = \frac{\beta I_0 L_{eff}}{1+x^2}$$

where $x = z/z_0$, in which $z_0 = \pi\omega_0^2/\lambda$ is the diffraction length of the beam, where ω_0 is the spot size at the focus, λ is the wavelength of the beam, and z is the sample position. I_0 is the input intensity at the focus z = 0 and equals the input energy divided by $\pi\omega_0^2$. $L_{eff} = (1 - e^{-\alpha L})/\alpha$ is the effective length, in which α is the linear absorption coefficient and L is the sample length.

2.2.8 Cell imaging

Cells were seeded in 24 glass bottom well plates at a density of $1x10^4$ cells per well and grown for 96 hours. For live cell imaging, the cells were incubated for 30 min in DMEM culture medium supplemented with 10% FCS, L-glutamine and Fungizone at 37 °C in an atmosphere of 5% CO_2 and 95% air. The cells were then washed with PBS (3 x 1 ml per well) and 1 ml of PBS was added to each well. The cells were imaged using a confocal laser scanning microscope.

2.2.9 Microscopy

For confocal microscopy, cells were imaged on a ZEISS LSM 710 META confocal laser-scanning microscope with a 63x and 100x oil lens. Image data acquisition and processing was performed using Zeiss LSM Image Browser, Zeiss LSM Image Expert and Image J. For real-time live cell imaging, the incubation chamber was connected to a ZEISS temperature control unit at 37 °C and a CO_2 controller with appropriate humidity. For transmission electron microscopy, cell samples were received pelleted in Eppendorf tubes. HepG2 cells were incubated with complex **Z4** (30 min) and then fixed in 3% glutaraldehyde and dehydrated in ethanol. The sections were examined using a FEI Tecnai Transmission Electron Microscope at an accelerating voltage of 80kV. Electron micrographs were taken using a Gatan digital camera.

For transmission electron microscopy, cell specimens were pre-incubated with **Z4** complex for 30 min and received pelleted in Eppendorf tubes. Fresh 3 % glutaraldehyde in 0.1 M phosphate buffer was added to re-suspend the pellet to ensure optimal fixation, and left overnight at 4 ˚C. The specimens were then washed in 0.1 M phosphate buffer at 4 ˚C, twice at 30 min intervals. Secondary fixation was carried out in 2 % aqueous osmium tetroxide for 2 hours at room temperature, followed by washing in buffer as above. Continuing at room temperature, this was followed by dehydration through a graded series of ethanol: 75 % (15 min), 95 % (15 min), 100 % (15 min) and 100 % (15 min). 100 % ethanol was prepared by drying over anhydrous copper sulphate for 15min. The specimens were then placed in an intermediate solvent, propylene oxide, for two changes of 15mins duration. . Resin infiltration was accomplished by placing the specimens in a 50/50 mixture of propylene oxide/Araldite resin. The specimens were left in this mixture overnight at room temperature. The specimens were left in full strength Araldite resin for 6-8 hrs at room temperature (with change of resin after 3-4 hrs) after which they were embedded in fresh Araldite resin for 48-72 hrs at 60 °C. Semi-thin sections approximately 0.5 μm thick were cut on a Leica

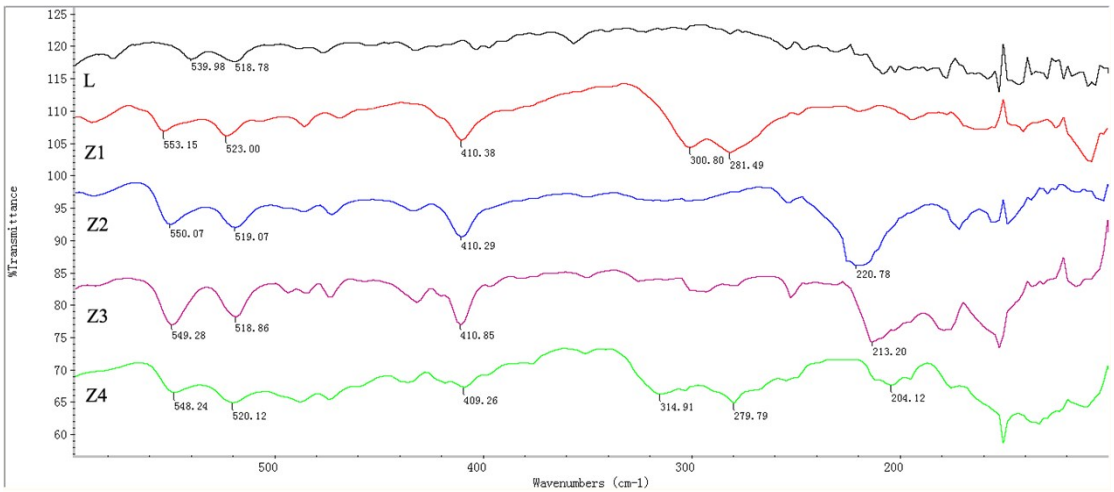

Fig. S1. Far IR spectra of L, Z1, Z2, Z3 and Z4.

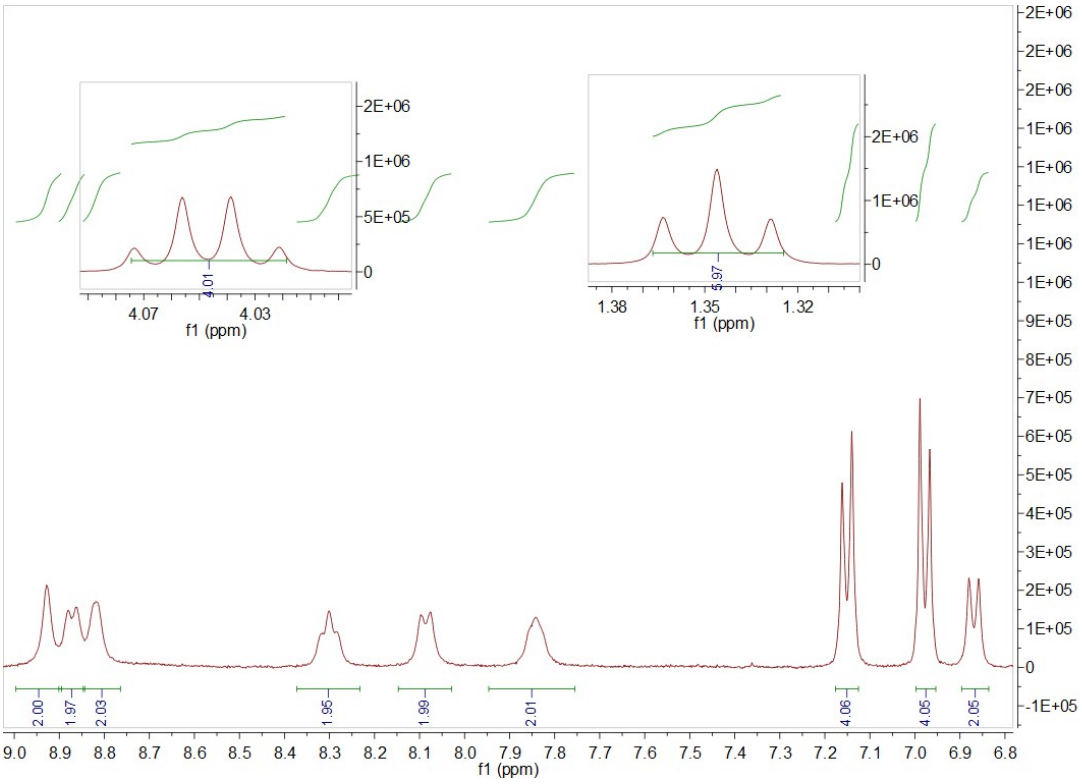

Fig. S2a. ^{1}H NMR spectrum of **Z1** (in DMSO-d_6).

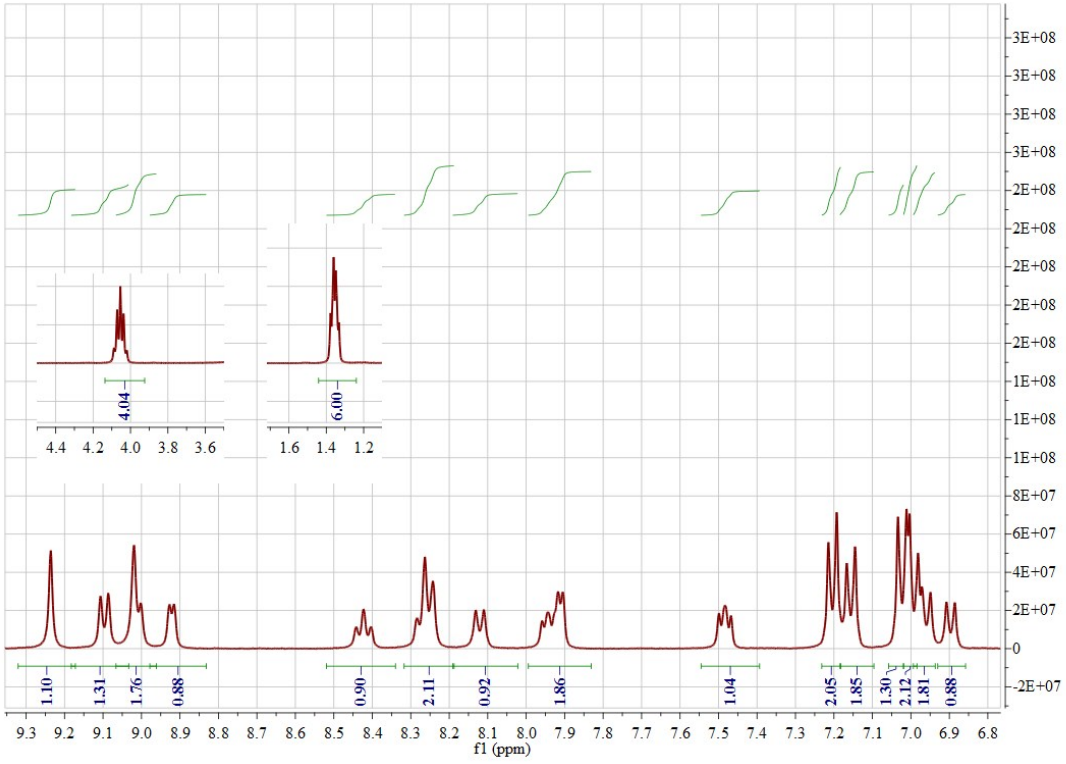

Fig. S2b. ^{1}H NMR spectrum of **Z2** (in DMSO-d_6).

Fig. S2c. ^{1}H NMR spectrum of **Z3** (in DMSO-d_6).

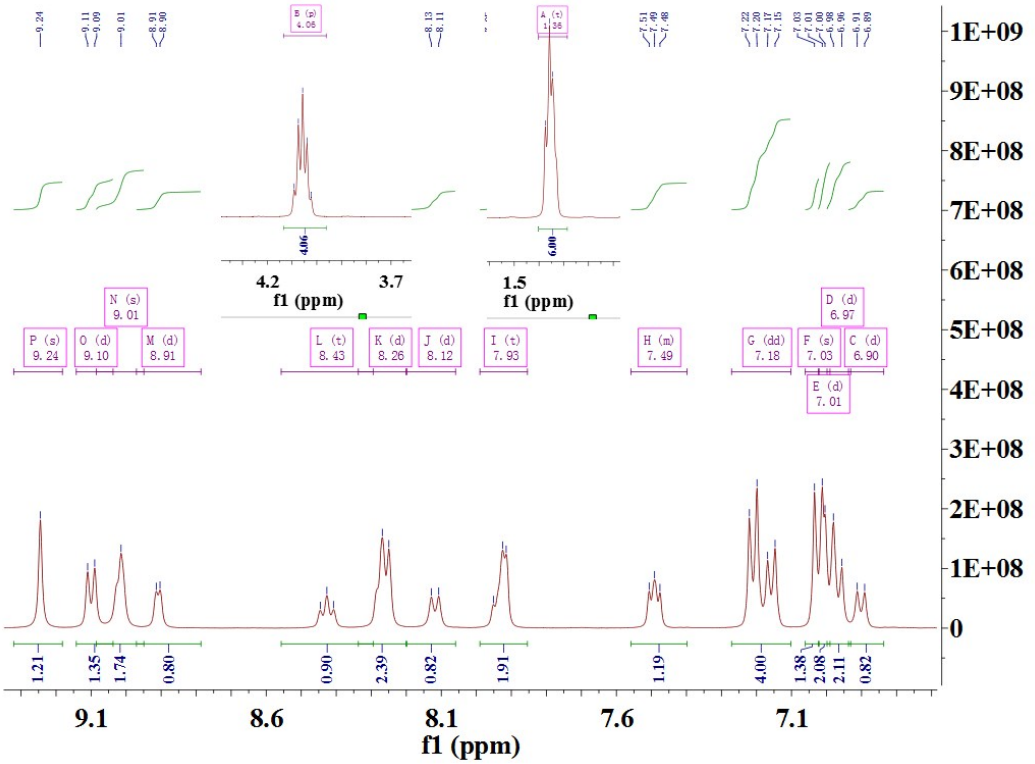

Fig. S2d. ^{1}H NMR spectrum of **Z4** (in DMSO-d_6).

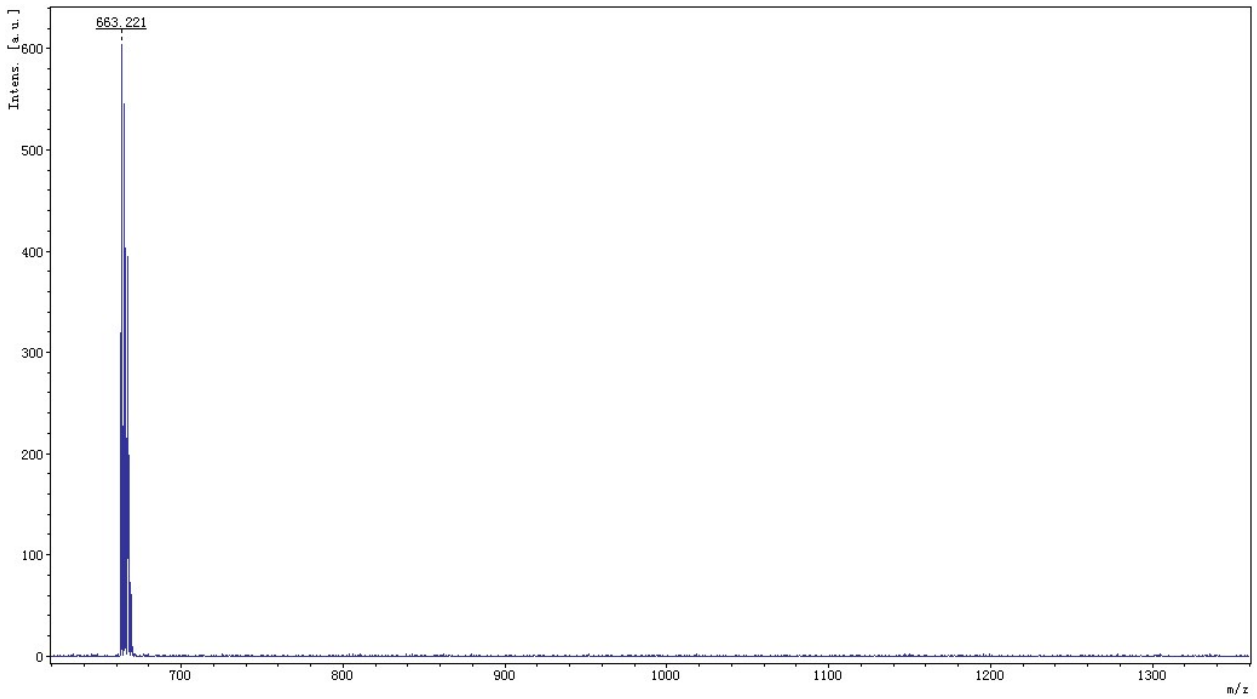

Fig. S3a. MALDI-TOF Mass spectra of **Z1.**

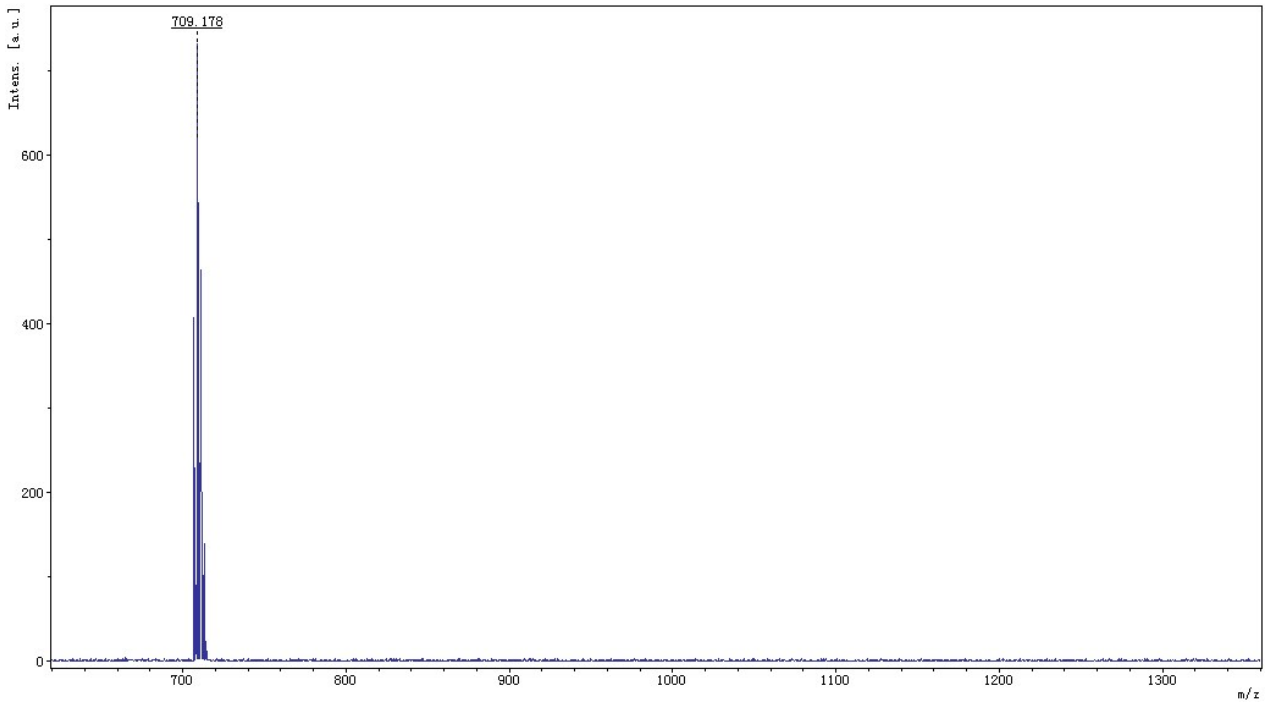

Fig. S3b. MALDI-TOF Mass spectra of **Z2.**

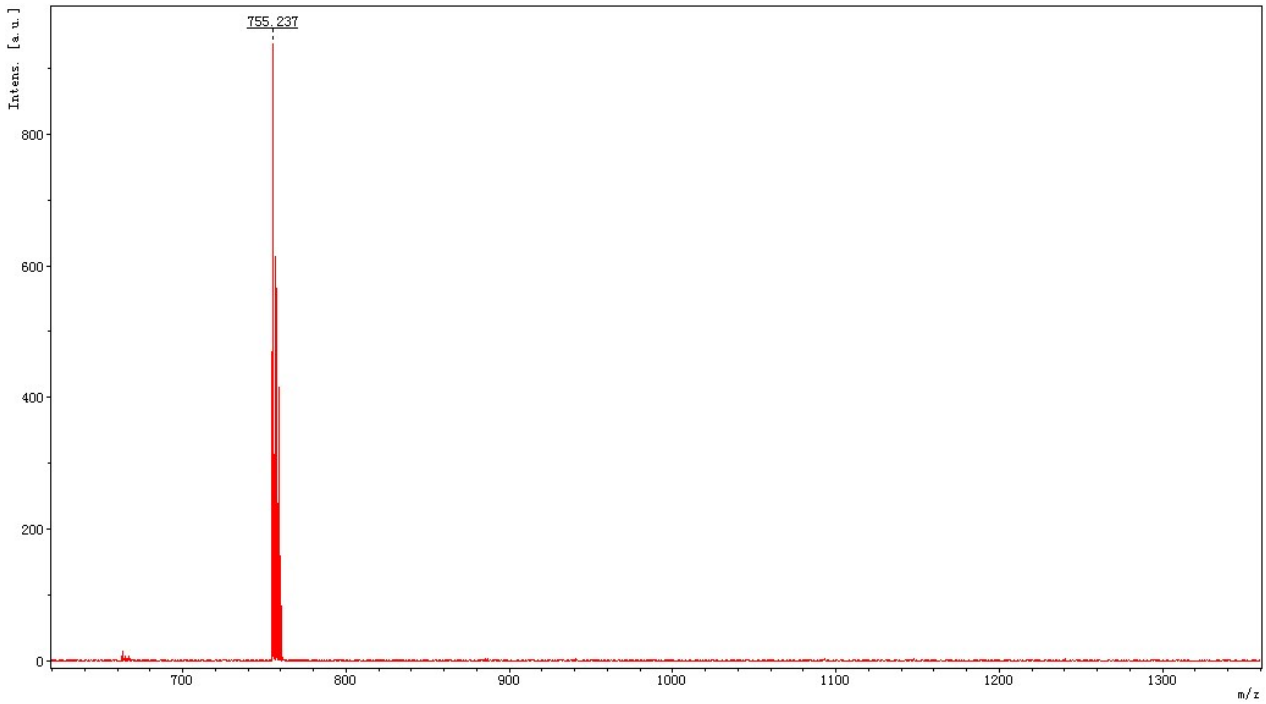

Fig. S3c. MALDI-TOF Mass spectra of **Z3.**

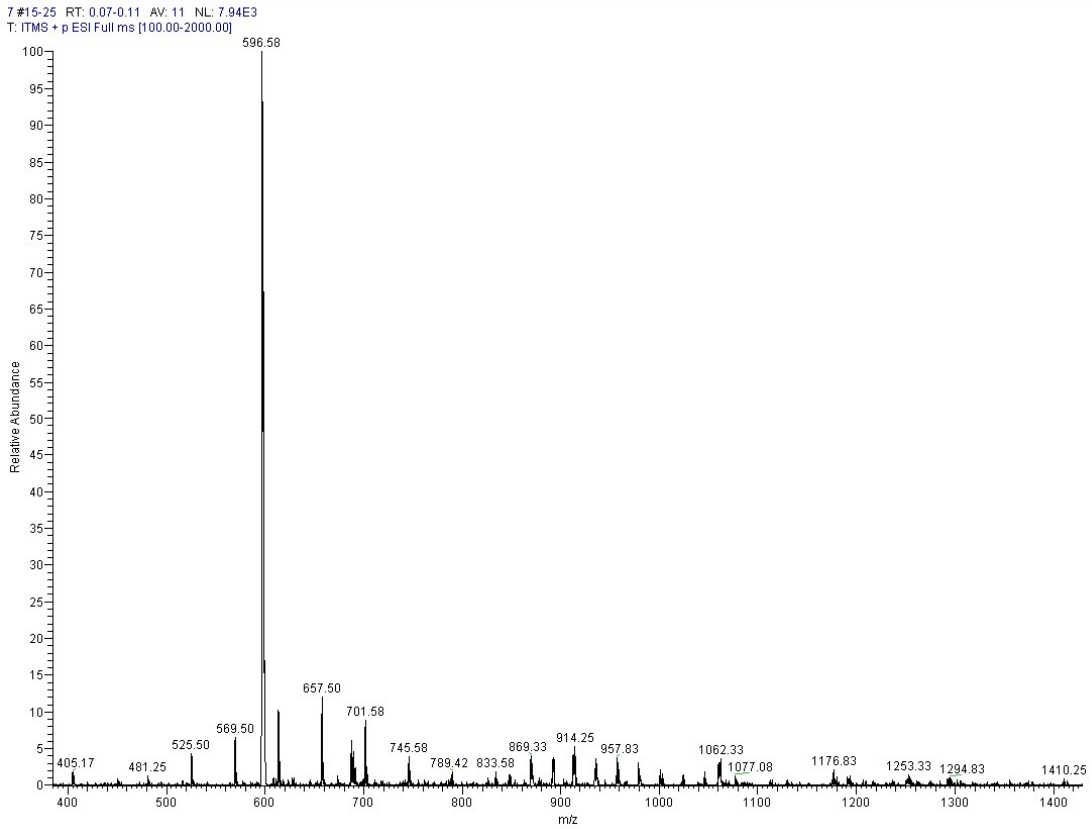

Fig. S3d. ESI-Mass spectrum of **Z4**.

Table S1. crystal data and structure refinement for **Z1**- **Z3**.

compound	**Z1**	**Z2**	**Z3**
Empirical formula	$C_{37}H_{32}Cl_2N_4O_2Zn$	$C_{37}H_{32}Br_2N_4O_2Zn$	$C_{37}H_{32}I_2N_4O_2Zn$
Formula weight	700.94	789.86	883.84
Temperature	298(2) K	298(2) K	298(2) K
Crystal system	Monoclinic	Monoclinic	Monoclinic
space group	$P2_1/c$	$P2_1/c$	$P2_1/c$
a [Å]	14.289(5)	14.164(5)	14.120(5)
b [Å]	14.212(5)	14.345(5)	14.552(5)
c [Å]	17.032(5)	17.368(5)	17.692(5)

α [°]	90.000(5)	90.000(5)	90.000(5)
β [°]	109.537(5)	108.597(5)	107.286(5)
γ [°]	90.000(5)	90.000(5)	90.000(5)
Volume [Å^3]	3259.6(19)	3344.6(19)	3471(2)
Z	4	4	4
Calculated density	1.428 Mg/m^3	1.569 Mg/m^3	1.691 Mg/m^3
Absorption coefficient	0.958 mm^{-1}	3.163 mm^{-1}	2.525 mm^{-1}
θ range [°]	1.51 to 25.00	1.88 to 25.00	1.51 to 25.00
Final R indices [I>2σ(I)]	R_1=0.0303 wR_2=0.0741	R_1=0.0387 wR_2=0.0696	R_1=0.0366 wR_2=0.1287
GOF	1.052	1.015	1.068

Table S2. Selected bond lengths (Å) and angles (°) for the crystal structure of **Z1-Z3**; selected bond lengths (Å) and angles (°) for the optimized structure of **Z4.**

Z1				**Z2**			
Distances		**Angles**		**Distances**		**Angles**	
Zn1-N2	2.099(17)	N2-Zn1-N3	73.88(6)	Zn1-N2	2.091(13)	N2-Zn1-N3	73.92(12)
Zn1-N3	2.219(18)	N2-Zn1-N4	74.23(6)	Zn1-N3	2.207(13)	N2-Zn1-N4	74.31(12)
Zn1-N4	2.218(19)	N3-Zn1-Cl1	96.68(15)	Zn1-N4	2.215(3)	N3-Zn1-Br1	97.03(9)
Zn1-Cl1	2.278(19)	N4-Zn1-Cl2	98.09(6)	Zn1-Br1	2.420(9)	N4-Zn1-Br2	98.72(9)
Zn1-Cl2	2.260(8)	Cl1-Zn1-C2	111.41(3)	Zn1-Br2	2.400(9)	Br1-Zn1-Br2	110.91(3)
Z3				**Z4**			
Distances		**Angles**		**Distances**		**Distances/Angles**	
Zn1-N2	2.089(4)	N2-Zn1-N3	73.95(14)	N2-Zn1	2.054	N8-Zn1	2.053
Zn1-N3	2.210(4)	N2-Zn1-N4	74.65(14)	N3-Zn1	2.184	N2-Zn1-N3	107.01
Zn1-N4	2.216(4)	N3-Zn1-I1	98.33(10)	N4- Zn1	2.182	N2-Zn1-N4	76.76
Zn1-I1	2.622(10)	N4-Zn1-I2	99.23(13)	N6- Zn1	2.196	N6-Zn1-N7	76.89
Zn1-I2	2.600(9)	Cl1-Zn1-I2	109.40(3)	N7- Zn1	2.198	N7-Zn1-N8	76.76

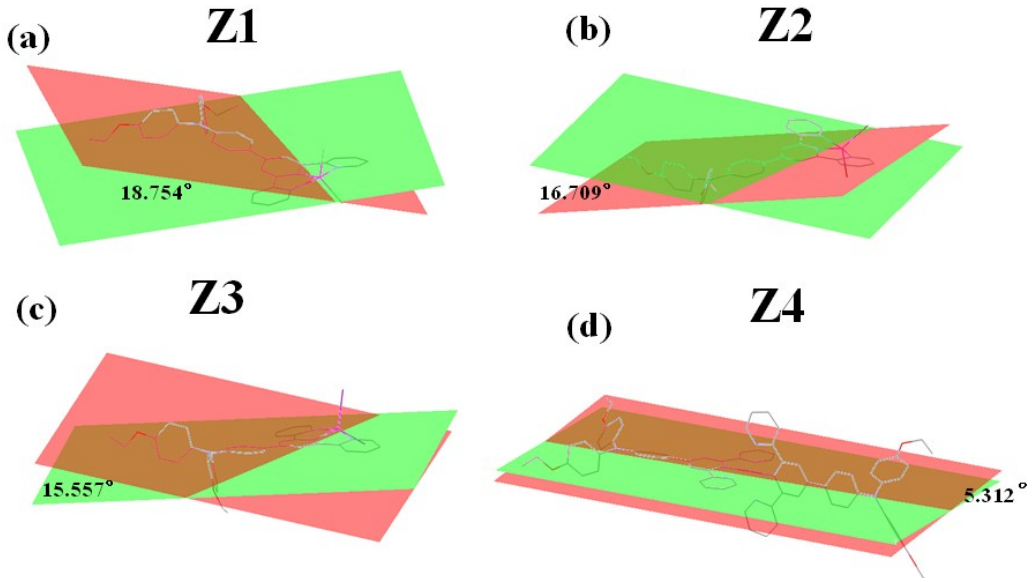

Fig. S4. The dihedral angles of **Z1**, **Z2** and **Z3** calculated by crystal structure, the dihedral angles of **Z4** calculated by optimized structure; H atoms are omitted for clarity.

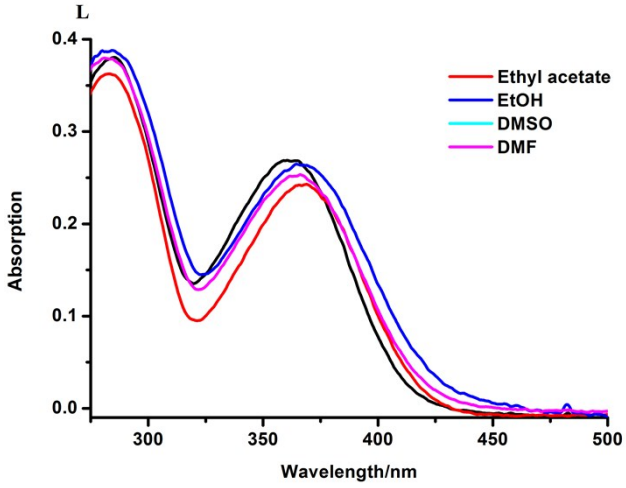

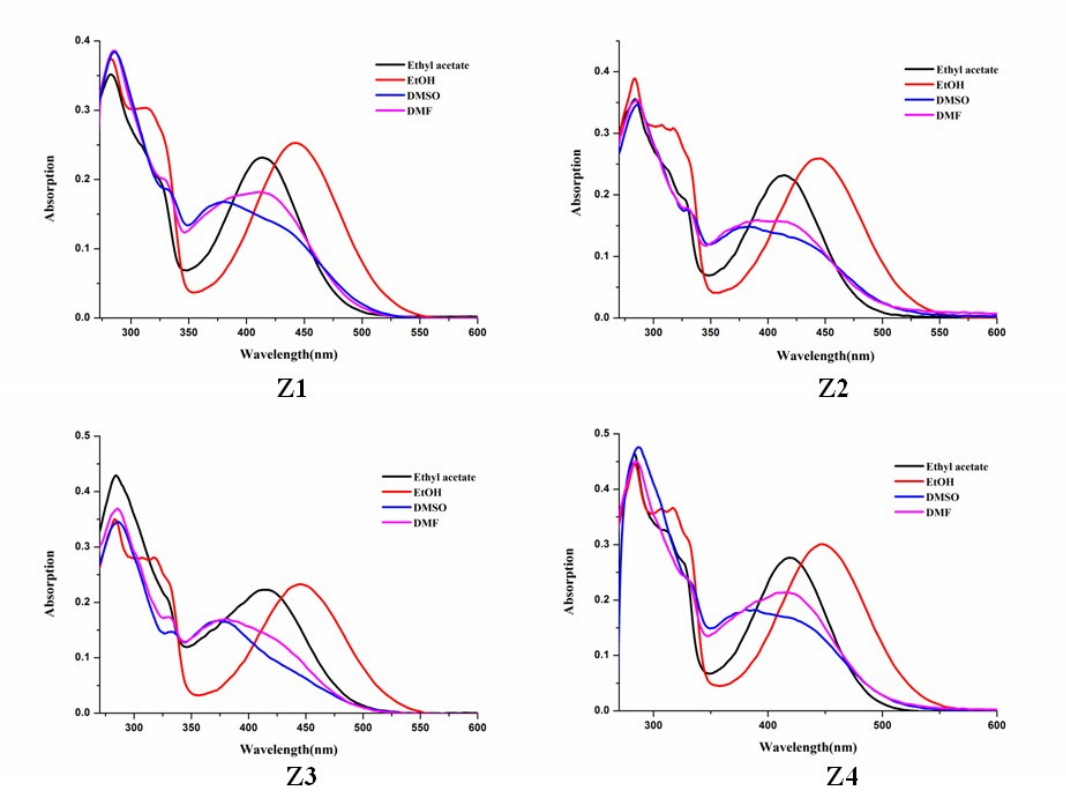

Fig. S5. Linear absorption spectra of the ligand **L** and the four complexes in different solvent with a concentration of 10 μM.

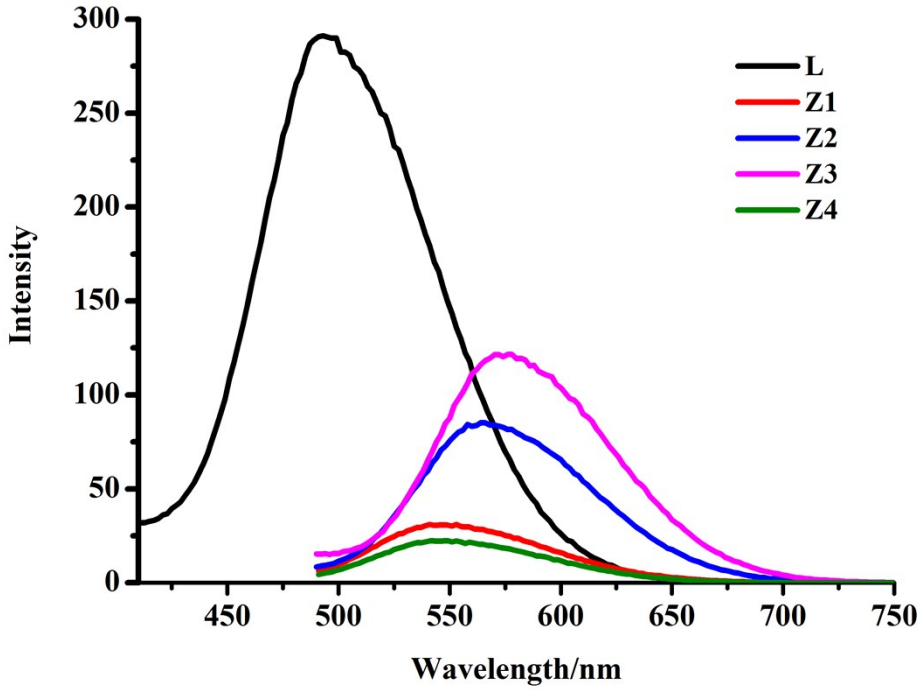

Fig. S6. The photoluminescence spectra of **L** and the four complexes in DMSO with a concentration of 10 μM.

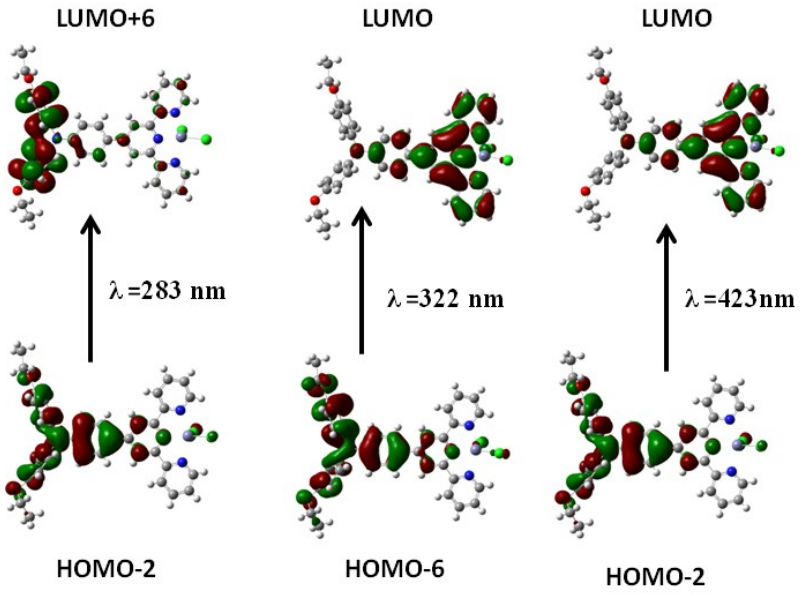

Fig. S7. The transition molecular orbital diagrams of the complex **Z1**.

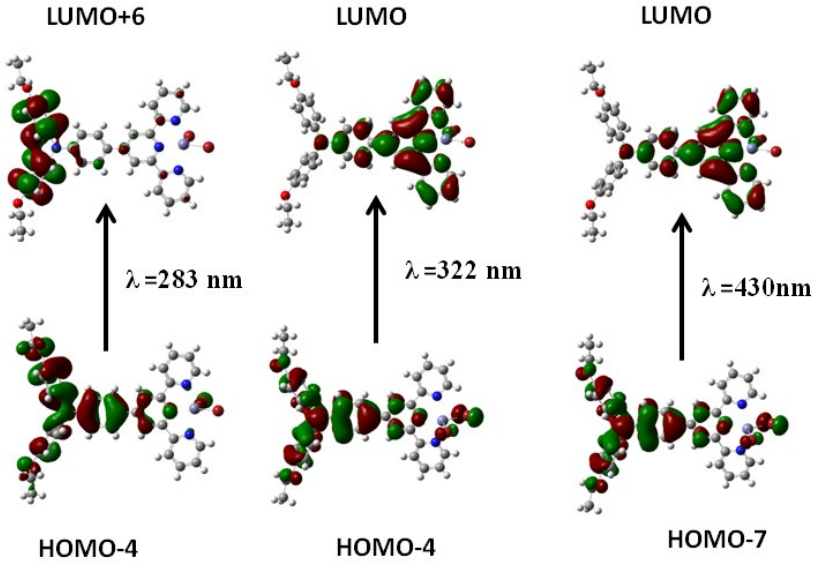

Fig. S8. The transition molecular orbital diagrams of the complex **Z2**.

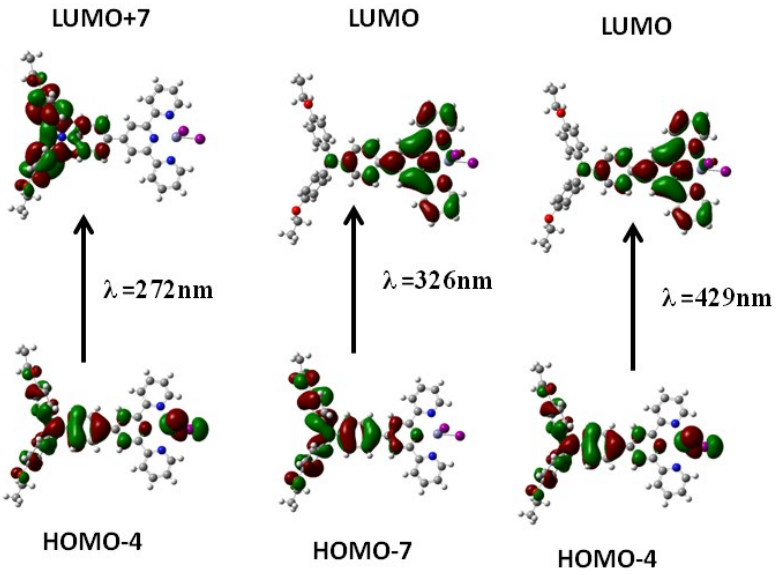

Fig. S9. The transition molecular orbital diagrams of the complex **Z3**.

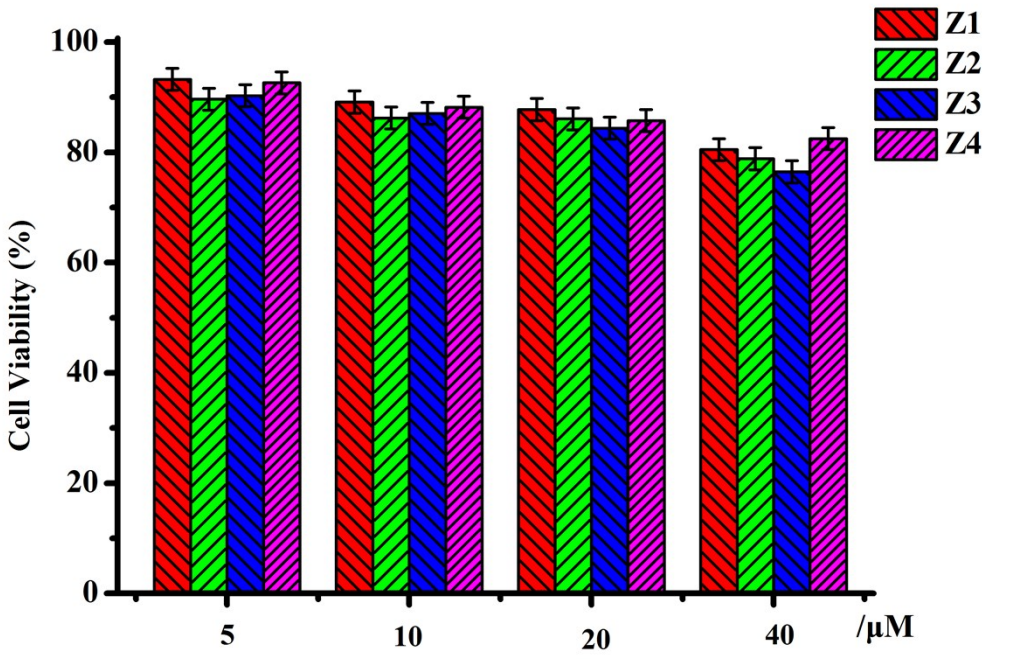

Fig. S10. MTT assay of HepG2 cells treated complex **Z1**-**Z4** in different concentration for 24 h.

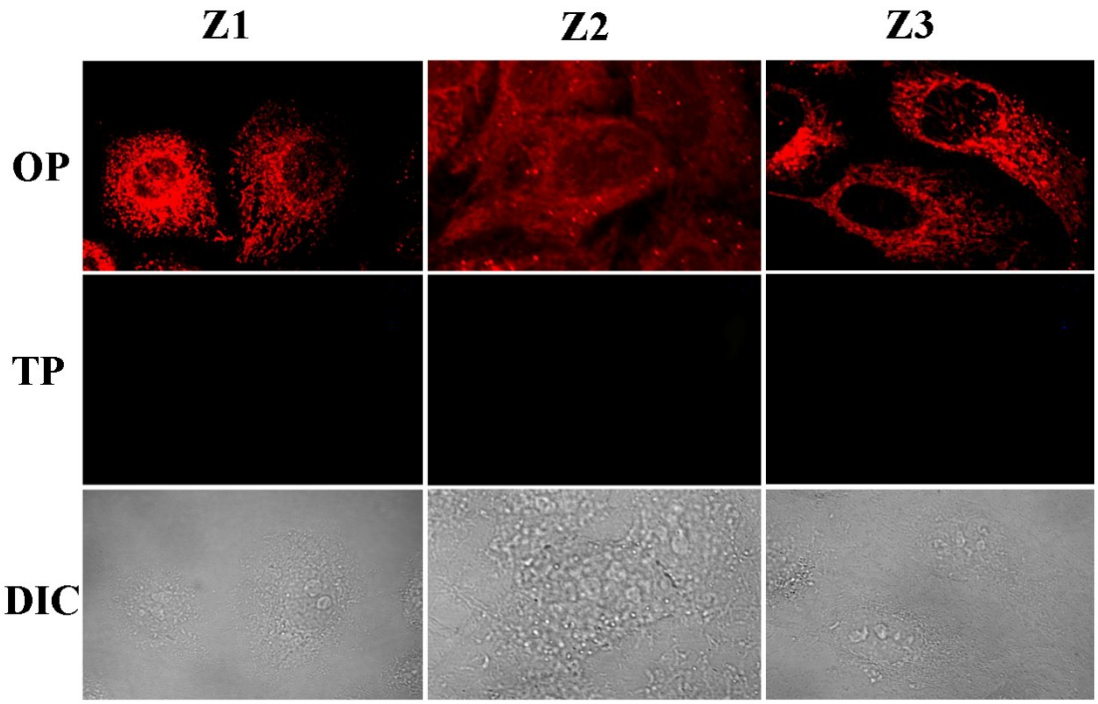

Fig. S11. One-photon and two-photon images of HepG2 cells incubated with **Z1**-**Z3** (λ_{ex} = 405 nm; λ_{ex} = 800 nm), All the scale bars represent at 20 μm.

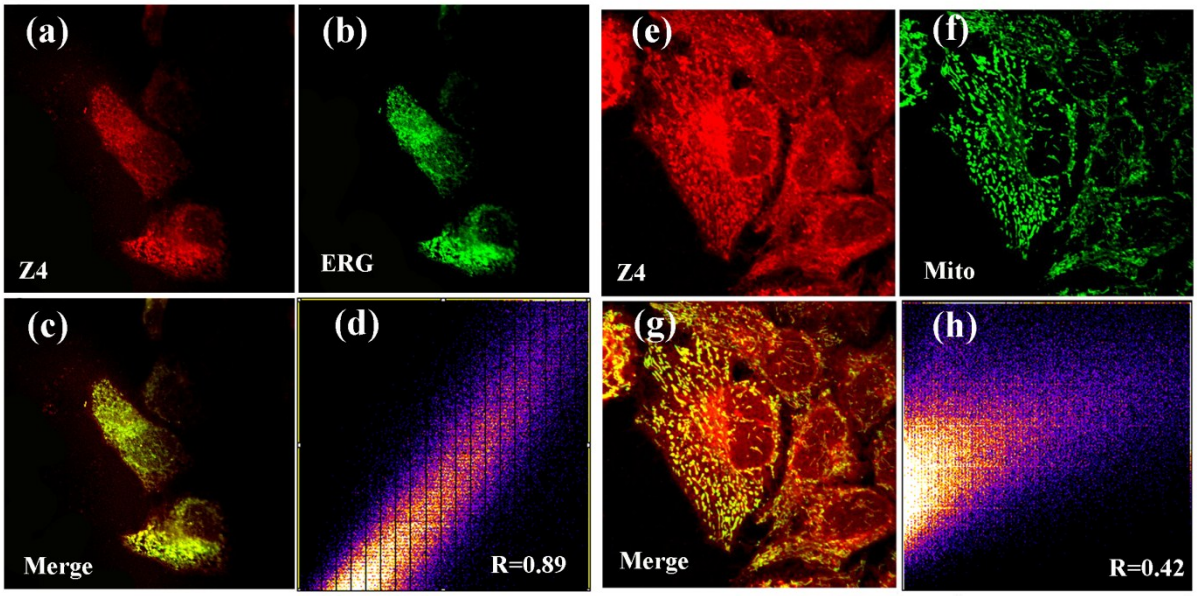

Fig. S12. (a-c) Confocal fluorescence image bright field images, and their overlay for living Hela cells incubated with 30μM of the **Z4** for 30 min at 37 °C, followed by incubation with 10 μM of ER -tracker™ green; (d) Pearson correlation coefficient profile of ROIs across HepG2 cells with **Z4** and ER -tracker™ green; (e-g) Confocal fluorescence image bright field images, and their overlay for living HepG2 cells incubated with 30μM of the **Z4** for 30 min at 37 °C, followed by incubation with 10 μM of Mito -tracker™ green; (h) Pearson correlation coefficient profile of ROIs across Hela cells with **Z4** and Mito -tracker™ green; All scale bars represent 20 μm.

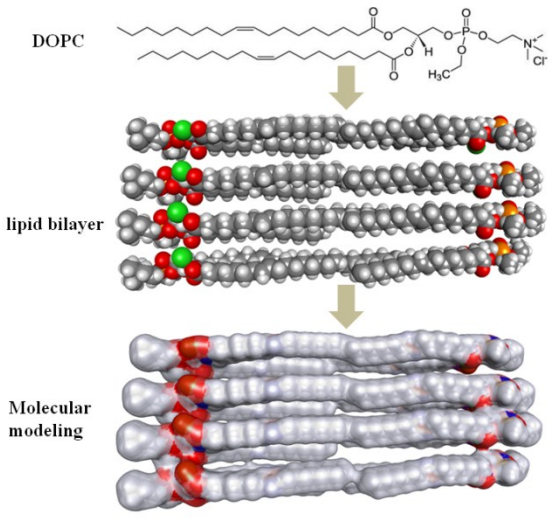

Fig. S13. The molecular simulation structure of corresponding lipid bilayer, based on the DOPC liposomes (DOPC = 1,2-dioleoyl-sn-glycero-3- phosphocholine).

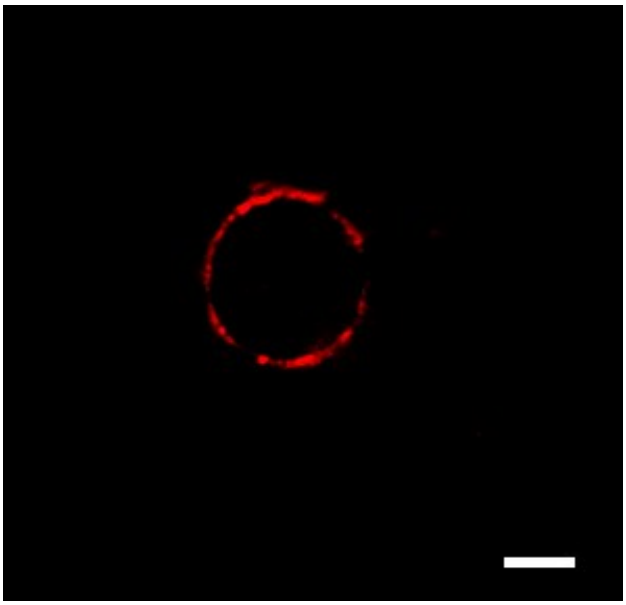

Fig. S14. Real-color fluorescence image of Ld GUVs stained with 4 μM Z4 ((λex = 800 nm, λem = 520-620 nm), bar = 10 μm

Reference:

Frisch, M.J., Trucks, G.W., Schlegel, H.B., Scuseria, G.E., Robb, M.A., Cheeseman, J.R., Gaussian 03 (Revision B.04). Wallingford, CT: Gaussion, Inc; 2004.

Xiao, L.F., Wang, H., Zhang, Q., Zhu, Y.Z., Luo, J.S., Liang, Y.K., Zhang, S.Y., Zhou, H.P., Tian, Y.P., Wu, J.Y,. 2015. Dyes & Pigments113, 165-173.

Zhang Q. Luo, J.S., Ye, L.L., Wang, H., Huang, B., Zhang, J., Wu, J.Y., Zhang, S.Y., Tian, Y.P., 2014. J. Mol. Struct. 1074, 33-42.